Progress In Electromagnetics Research, Vol. 117, 267–281, 2011

AN IMPROVED CUBIC POLYNOMIAL METHOD FOR INTERPOLATING/EXTRAPOLATING MOM MATRICES OVER A FREQUENCY BAND

W.-D. Li[1, *], J.-X. Miao[2], J. Hu[1], Z. Song[1], and H.-X. Zhou[1]

[1]State Key Laboratory of Millimeter Waves, School of Information Science and Engineering, Southeast University, Nanjing 210096, P. R. China

[2]School of Applied Mathematics, Nanjing University of Finance and Economics, Nanjing 210046, P. R. China

Abstract—The inter/extrapolation accuracy of the cubic polynomial method has been improved by optimizing three frequency samples for frequency-sweeping in the method of moments (MoM). In the method, the frequency samples are optimized by minimizing the global maximum of the polynomial component at the stationary points and two terminal points of the frequency band. The optimal frequency samples can be expressed as analytical forms of the two terminal points. Numerical examples are presented to validate the proposed method through comparison with the Padé approximation.

1. INTRODUCTION

The method of moments (MoM)-based surface integral equation solver has been a tool in wide use for analyzing time-harmonic electromagnetic (EM) radiation and scattering from perfect electrically conducting (PEC) objects [1, 2]. The MoM results in a dense impedance matrix, and the MoM matrix is computationally intensive especially for frequency-sweeping cases. The polynomial interpolation and extrapolation methods [3–12, 19], the rational polynomial approaches [13–18, 20], and other techniques [21–27] have been proposed for fast generating the MoM matrices, the current distributions, and the radar-cross-section (RCS) results over a frequency band. The quadric polynomial interpolation method

Received 10 May 2011, Accepted 1 June 2011, Scheduled 9 June 2011

* Corresponding author: Wei-Dong Li (wdli@emfield.org).

originally adopted in [3] was improved by extracting the dominant phase term [4]. A cubic polynomial interpolation scheme with derivative term was proposed in the authors' previous work [11]. In this scheme, the modified matrix element consists of the remaining phase term and the quadratic polynomial term of the normalized frequency, and it is more suitable for polynomial interpolation than the version in [4]. The position of the internal frequency sample is optimized. Hence, this scheme yields more accurate matrices over the frequency band than the schemes in [4] and [10]. However, the positions of the first and third frequency samples still need to be optimized within the frequency band. In [13–16], the rational polynomial approaches such as the Padé approximation have been developed to fast obtain the current distributions or the far field results over a frequency band. Compared with the matrix element, these parameters vary drastically with frequency [4], respectively. Hence, a number of frequency data and frequency-derivative data are needed to obtain the coefficients of the approaches, respectively.

In this paper, a cubic polynomial inter/extrapolation method is investigated for efficiently generating MoM matrices over a frequency band. The method is the improved version of the previous work [11], and its significant difference is that the positions of all three frequency samples are optimized within the frequency band by minimizing the amplitude of the polynomial component and they can be expressed as analytical forms of two terminal points of the frequency band. The lowest and highest frequency samples define one sub-band. The matrices inside and outside the sub-band are generated via interpolation and extrapolation, respectively.

The rest of this paper is organized as follows. In Section 2, a cubic polynomial inter/extrapolation method is described in detail. Section 3 provides numerical examples to validate the proposed method. Some conclusions are given in Section 4.

2. CUBIC POLYNOMIAL INTER/EXTRAPOLATION SCHEME WITH THREE OPTIMAL FREQUENCY SAMPLES

The electric field integral equation (EFIE) or the combined field integral equation (CFIE) is used to analyze the 3D EM problem from PEC objects in a free space [1]. The surface current density $\mathbf{J}$ induced by the incident time-harmonic EM field is expanded in terms of the RWG functions [2]. After the Galerkin's procedure, the EFIE-MoM or CFIE-MoM impedance matrix at each frequency $f \in [f_l, f_h]$ is yielded. For simplicity, we denote by Z_{mn} the matrix element (10)

(or (12)) in the frequency-sweeping case [11]. The modified matrix element employed here is

$$\tilde{Z}_{mn} = Z_{mn} f_r e^{j2\pi f_r R_{mn}}, \tag{1}$$

where $f_r = f/f_h$ is the normalized frequency and varies from f_l/f_h to 1, and R_{mn} is the distance between the centers of the RWG elements S_m and S_n in the electrical size at f_h.

As elucidated in [11], $\tilde{Z}_{mn}$ is a product of a quadratic polynomial in f_r and the remaining phase term. Compared with the quadratic polynomial, the cubic polynomial may effectively mitigate the negative effect of the remaining term on the inter/extrapolation accuracy. In [11], the optimal position of the second frequency sample is located, however the positions of the first and third frequency samples still need to be optimized.

The scheme under investigation involves three frequency samples f_i $(i = 0, 1, 2)$ within $[f_l, f_h]$ and the matrices at the normalized frequencies $x_i = f_i/f_h$ $(i = 0, 1, 2)$ as well as the first derivative at x_1. The inter/extrapolation formula for each f_r in $[f_l/f_h, 1]$ is expressed as

$$\tilde{Z}^A_{mn}(f_r) = \sum_{i=0}^{2} y_i \phi_i(f_r) + y'_1 \varphi_1(f_r), \tag{2}$$

where y_i is $\tilde{Z}_{mn}$ at x_i for $i = 0, 1, 2$, and y'_1 is $\tilde{Z}'_{mn}$ at x_1; $\phi_i(f_r)$ $(i = 0, 1, 2)$ and $\varphi_1(f_r)$ have been defined in [11]. Its remainder term is given by

$$\tilde{Z}_{mn} - \tilde{Z}^A_{mn}(f_r) = \frac{\tilde{Z}^{(4)}_{mn}(\xi)}{4!} W(x_0, x_1, x_2, f_r), \tag{3}$$

where ξ lies in $(f_l/f_h, 1)$, and

$$W(x_0, x_1, x_2, f_r) = (f_r - x_0)(f_r - x_1)^2(f_r - x_2). \tag{4}$$

Let

$$t = \frac{f_r - f_l/f_h}{1 - f_l/f_h}, \tag{5}$$

t_i is obtained by substituting x_i into (5) for $i = 0, 1, 2$. Then,

$$W(x_0, x_1, x_2, f_r) = (1 - f_l/f_h)^4 U(t_0, t_1, t_2, t), \tag{6}$$

where t varies within $[0, 1]$, and

$$U(t_0, t_1, t_2, t) = (t - t_0)(t - t_1)^2(t - t_2). \tag{7}$$

The error norm is defined, for indicating the inter/extrapolation error of matrix, as

$$error(f_r) = \frac{||\tilde{Z} - \tilde{Z}^A||_F}{||\tilde{Z}||_F}, \tag{8}$$

where $||\cdot||_F$ denotes the Frobenius norm of matrix. By using (3) and (6), (8) is rewritten as

$$error(f_r) = \text{coeff}(t_0, t_1, t_2, f_r)(1 - f_l/f_h)^4 |U(t_0, t_1, t_2, t)|, \quad (9)$$

where the error coefficient is

$$\text{coeff}(t_0, t_1, t_2, f_r) = \frac{||\tilde{Z}^{(4)}(\{\xi\})||_F}{4!||\tilde{Z}||_F}, \quad (10)$$

and $\{\xi\}$ denotes the set of ξ in (3).

We have investigated extensive numerical examples for analyzing the frequency response of (8) and (10), respectively. Without loss of generality, a PEC sphere of radius 1 cm is considered. Seen from Figure 1, the error norm varies drastically with the positions of the frequency samples and the operating frequency, and the error coefficient is not sensitive to (t_0, t_1, t_2) and f_r. It is practical to minimize $\max\limits_{t\in[0,1]} |U(t_0, t_1, t_2, t)|$ by optimizing (t_0, t_1, t_2).

Section 3 in [11] shows that $\max\limits_{f_r\in[x_0,x_2]} |W(x_0, x_1, x_2, f_r)|$ attains the minimum when $x_1 = (x_0 + x_2)/2$, which means that $\max\limits_{t\in[t_0,t_2]} |U(t_0, t_1, t_2, t)|$ attains the minimum when $t_1 = (t_0 + t_2)/2$. Hence, we minimize $\max\limits_{t\in[0,1]} |U(t_0, t_1, t_2, t)|$ by optimizing (t_0, t_2) over $\Omega = [0, 1] \times [0, 1]$.

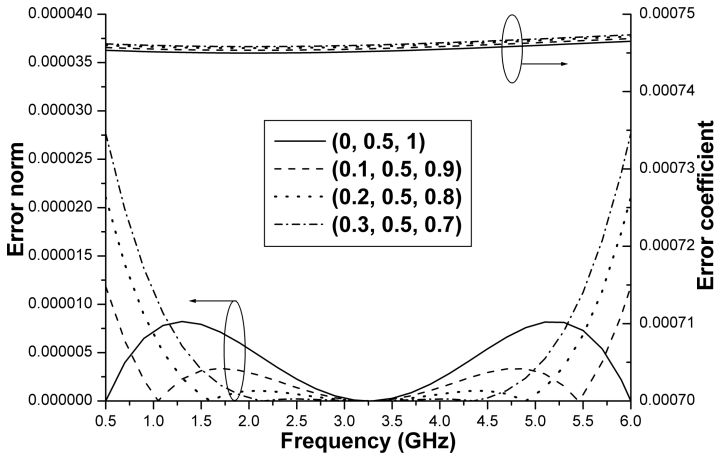

Figure 1. Frequency response of the error norm and the error coefficient for the sphere obtained from (2) with different choices of (t_0, t_1, t_2) in the EFIE case, respectively.

Since the stationary points of $|U(t_0, t_1, t_2, t)|$ with t over $[0, 1]$ are $t_1^{\pm} = t_1 \pm (t_2 - t_0)\sqrt{2}/4$ and t_i $(i = 0, 1, 2)$, the minimum of $\max_{t\in[0,1]} |U(t_0, t_1, t_2, t)|$ with (t_0, t_2) over Ω can be expressed as

$$\min_{(t_0,t_2)\in\Omega} \max \left\{ |U(t_0, t_1, t_2, 0)|, |U(t_0, t_1, t_2, 1)|, |U(t_0, t_1, t_2, t_1^{\pm})| \right\}. \quad (11)$$

After solving (11) (see the Appendix), the optimal values of t_0 and t_2 can be expressed as

$$t_0 = \frac{1}{2}\left(1 - \sqrt{2}\sqrt{\sqrt{2} - 1}\right), \quad t_2 = \frac{1}{2}\left(1 + \sqrt{2}\sqrt{\sqrt{2} - 1}\right) \quad (12)$$

and $\max_{t\in[0,1]} |U(t_0, t_1, t_2, t)|$ attains the minimal value of $(\sqrt{2}-1)^2/16$. As a result, (9) is less than or equal to

$$\text{coeff}(t_0, t_1, t_2, f_r)(1 - f_l/f_h)^4 \left(\sqrt{2} - 1\right)^2 /16. \quad (13)$$

When $(t_0, t_1, t_2) = (0, 0.5, 1)$, $\max_{t\in[0,1]} |U(t_0, t_1, t_2, t)|$ attains the minimal value of $1/64$, which is the case in [11]. Then, (9) is less than or equal to

$$\text{coeff}(0, 0.5, 1, f_r)(1 - f_l/f_h)^4/64. \quad (14)$$

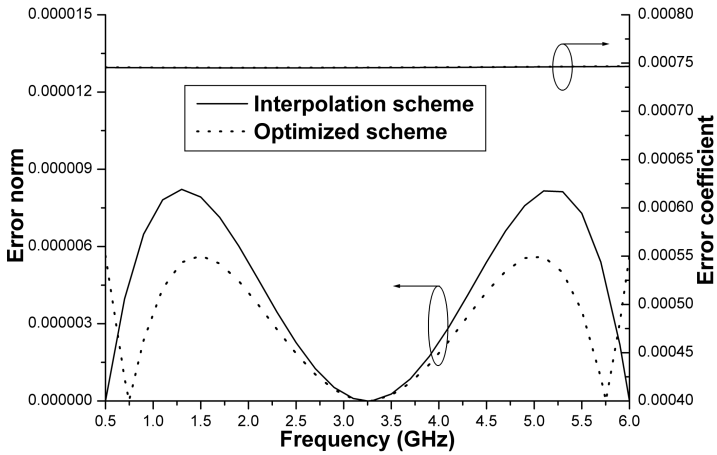

Figure 2. Frequency response of the error norm and the error coefficient for the sphere obtained from the different schemes in the EFIE case, respectively.

The Equations (5) and (12) show that the optimal frequency samples can be expressed as analytical forms of f_l and f_h, and they are all located inside $[f_l, f_h]$. In this way, the range between the lowest and highest frequency samples is one sub-band of $[f_l, f_h]$. By using (2), the matrices inside and outside the sub-band are generated via interpolation and extrapolation, respectively.

Figures 2 and 3 plot the error norms and the error coefficients for the optimized scheme and the interpolation scheme with $(t_0, t_1, t_2) = (0, 0.5, 1)$, respectively, in the EFIE and CFIE cases. The error

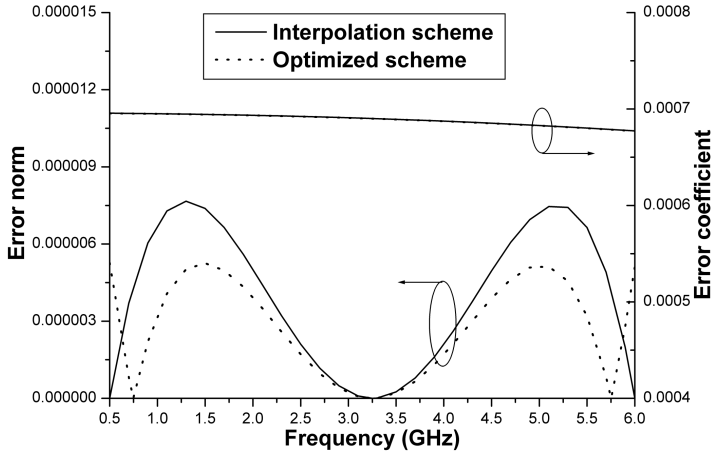

Figure 3. Frequency response of the error norm and the error coefficient for the sphere obtained from the different schemes in the CFIE case, respectively.

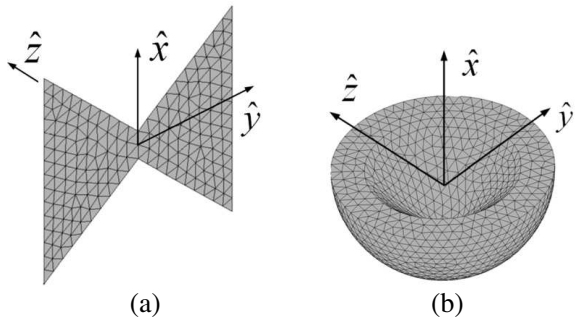

Figure 4. Two PEC objects. (a) Model of bowtie; (b) hemisphere with cone cavity.

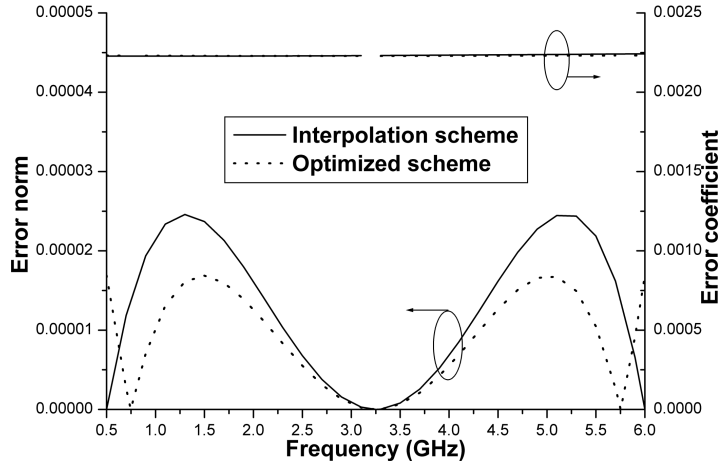

Figure 5. Frequency dependence of the error norm and the error coefficient for the model of bowtie obtained from the different schemes, respectively.

coefficients for the two schemes are almost identical to each other, and the error norm for the optimized scheme is less than that for the interpolation scheme. From (13) and (14), it is easily known that the error norm for the optimized scheme is reduced to about 68.63% of that for the interpolation scheme.

A model of bowtie with edge 7.5 cm is investigated as shown in Figure 4(a), where 422 unknowns are involved. In Figure 5, the error norm for the optimized scheme is less than that for the interpolation scheme. The reason is the same as in the above case.

In the optimized scheme, the inter/extrapolation error of matrix is a product of the error coefficient and the polynomial component. The error coefficient is not sensitive to the positions of the frequency samples and the operating frequency, and the frequency behavior of the inter/extrapolation error of matrix is closely related to the polynomial component. Hence, it is practical to minimize the amplitude of the polynomial component rather than the inter/extrapolation error of matrix by optimizing the frequency samples. The above approach offers a practical guideline to locate the optimal frequency samples.

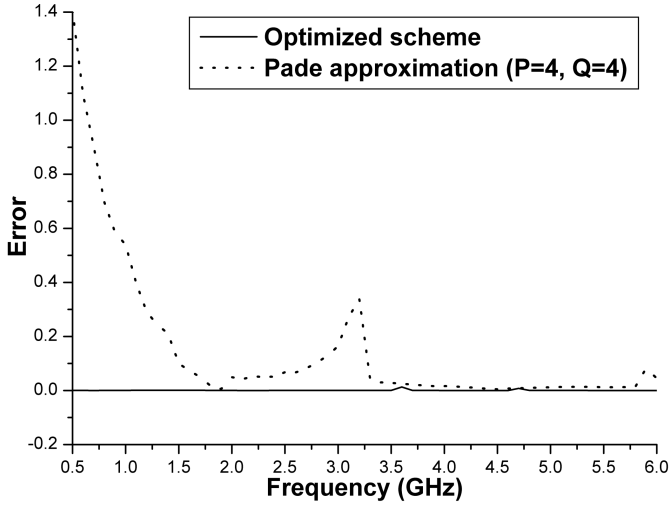

Figure 6. Error of the current distributions for the model of bowtie obtained from the optimized scheme and the Padé approximation, respectively. Here, P and Q denote the polynomial degrees of the numerator and denominator in the Padé approximation, respectively, and the frequency increment is 0.1 GHz.

3. NUMERICAL EXAMPLES

In this section, the inter/extrapolation scheme optimized in (12) is tested on the two objects of Figures 4(a) and (b) through comparison with the MoM and the Padé approximation [14]. The incident wave is a $\hat{y}$-polarized plane wave propagating along $\hat{z}$-axis. The EFIE and CFIE equations are applied to the open and close objects, respectively. All the calculations are carried out on a Xeron computer with 2.5 GHz.

The first example is the model of bowtie as elucidated in Section 2. The current distributions and the monostatic RCS are calculated through the optimized scheme, the Padé approximation (with the expanded points of 1.875 and 4.625 GHz), and the MoM, respectively. Figure 6 shows that the optimized scheme yields more accurate current distributions than the Padé approximation. Here, the error is defined as the ratio of the difference between the results obtained from the MoM and one of the other methods to the results from the MoM. The Padé approximation yields the results deviating from those from the MoM at the low and middle frequency ranges. In Figure 7, the monostatic RCS results from the optimized scheme are in good agreement with those from the MoM and the results from the Padé approximation are not.

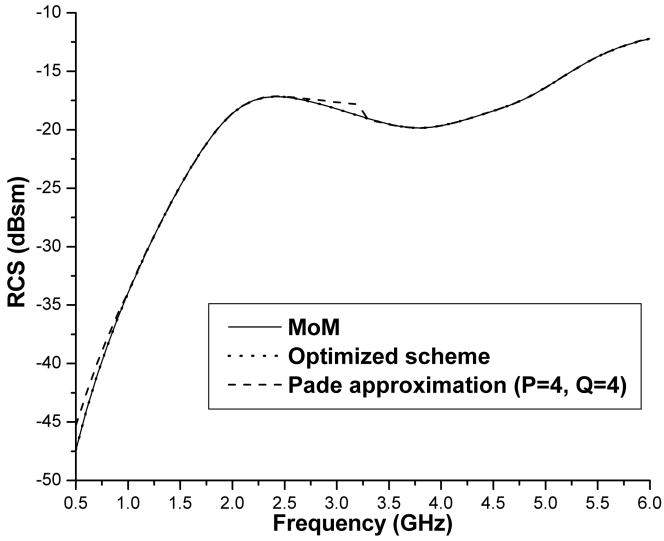

Figure 7. Frequency response of the monostatic RCS for the model of bowtie obtained from the optimized scheme and the Padé approximation, respectively.

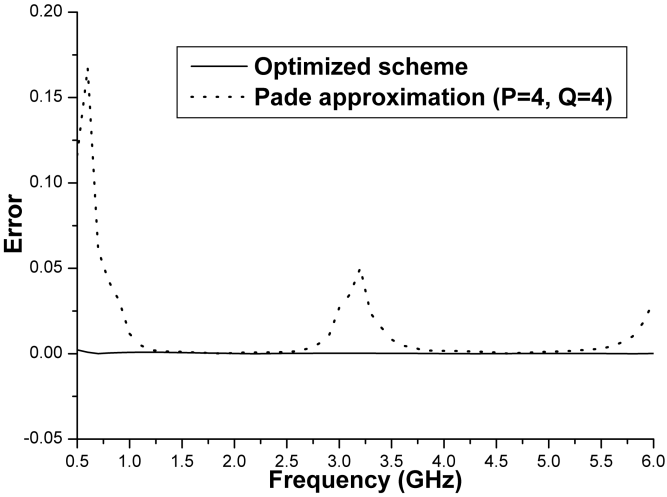

Figure 8. Error of the current distributions for the model of the hollow hemisphere obtained from the optimized scheme and the Padé approximation, respectively.

The second example is a hemisphere with cone cavity as shown in Figure 4(b), where the radius of the hemisphere is 5 cm and the radius and depth of the cone cavity are 3.5 cm, respectively. The surface is discretized into 2426 triangles with 3639 unknowns. The errors of the current distributions from the optimized scheme and the Padé approximation are plotted in Figure 8, respectively, and the monostatic RCS results plotted in Figure 9, respectively. The Padé approximation (with the expanded points of 1.875 and 4.625 GHz) gives less accurate results than the optimized scheme.

Listed in Table 1 is the CPU time for solving the current

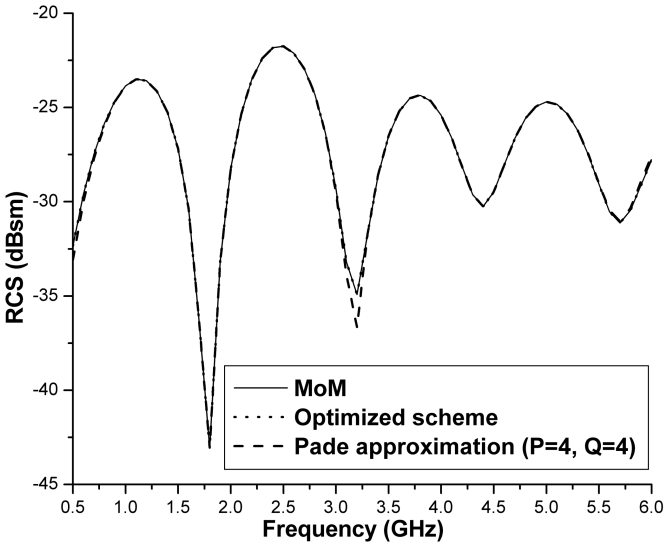

Figure 9. Frequency response of the monostatic RCS for the hollow hemisphere obtained from the optimized scheme and the Padé approximation, respectively.

Table 1. CPU time for solving the current distributions at 56 frequencies for the hemisphere with cone cavity used in the different methods (in minutes).

	Optimized	Padé	MoM
Matrices at frequency samples	133.64	601.36	1870.09
Inter/extrapolation of matrices or currents	1.84	0.029	/
Iteration solution	20.54	6.60	20.47
Total time	156.02	607.99	1890.56

distributions at 56 frequencies used in the optimized scheme, the Padé approximation, and the MoM, respectively. The CPU time for calculating and inter/extrapolating the matrices used in the optimized scheme is 22.53% of that used in the Padé approximation and 7.24% of that used in the MoM. The total CPU time used in the optimized scheme is much less than that used in the other methods, respectively, though the iteration time used in the optimized scheme is the largest.

4. CONCLUSION

In this paper, a cubic polynomial inter/extrapolation method is improved for efficiently generating the MoM matrices over a frequency band. The frequency samples employed are optimized by minimizing the amplitude of the polynomial component of the error norm. The optimized scheme yields more accurate current distributions and far-field results over the frequency band than the Padé approximation.

ACKNOWLEDGMENT

This work was supported in part by NSFC under Grant 60901013 and 60921063, in part by National 973 projects under Grant 2010CB327400 and 2009CB320203, in part by National High-Tech Research Plan of China under Grant 2008AA01Z223 and 2009AA011503, in part by the Scientific Research Foundation for the Returned Overseas Chinese Scholars, State Education Ministry, and in part by Innovation Project Program of State Key Laboratory of Millimeter Waves under Grant Z201006.

APPENDIX A.

Let

$$\Psi_{\mathrm{I}}(x,y) = (y-x)^4/64, \tag{A1}$$

$$\Psi_{\mathrm{II}}(x,y) = (1-x)(2-x-y)^2(1-y)/4, \tag{A2}$$

$$\Psi_{\mathrm{III}}(x,y) = x(x+y)^2y/4, \tag{A3}$$

and then we define over the domain $\Omega = [0,1] \times [0,1]$

$$\varpi(x,y) = \max\left\{\Psi_{\mathrm{I}}(x,y), \Psi_{\mathrm{II}}(x,y), \Psi_{\mathrm{III}}(x,y)\right\}. \tag{A4}$$

The focus of the appendix is to minimize $\varpi(x,y)$ by optimizing the point (x,y) over Ω.

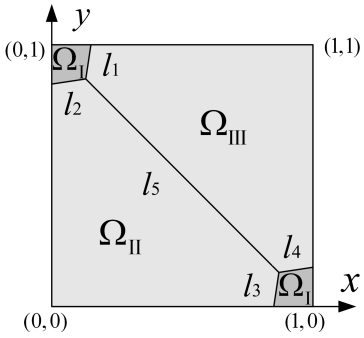

Figure A1. Sub-domains separated by the lines l_i $(i = 1, 2, \ldots, 5)$.

The function $\varpi(x, y)$ is continuous in Ω and can be further expressed as

$$\varpi(x,y) = \begin{cases} \Psi_{\mathrm{I}}(x,y), & (x,y) \in \Omega_{\mathrm{I}}, \\ \Psi_{\mathrm{II}}(x,y), & (x,y) \in \Omega_{\mathrm{II}}, \\ \Psi_{\mathrm{III}}(x,y), & (x,y) \in \Omega_{\mathrm{III}}, \end{cases} \tag{A5}$$

where Ω_{I}, Ω_{II}, and Ω_{III} are separated by the following lines l_i $(i = 1, 2, \ldots, 5)$ in Figure A1:

$$\begin{aligned} l_1 &: \; x = y\left(5 + 4\sqrt{2} - 2\sqrt{14 + 10\sqrt{2}}\right), \\ l_2 &: \; 1 - y = (1 - x)\left(5 + 4\sqrt{2} - 2\sqrt{14 + 10\sqrt{2}}\right), \\ l_3 &: \; 1 - y = (1 - x)\left(5 + 4\sqrt{2} + 2\sqrt{14 + 10\sqrt{2}}\right), \\ l_4 &: \; x = y\left(5 + 4\sqrt{2} + 2\sqrt{14 + 10\sqrt{2}}\right), \\ l_5 &: \; x + y = 1. \end{aligned}$$

In fact, l_2 and l_3 are solutions to $\Psi_{\mathrm{I}}(x, y) = \Psi_{\mathrm{II}}(x, y)$, and l_1 and l_4 are solutions to $\Psi_{\mathrm{I}}(x, y) = \Psi_{\mathrm{III}}(x, y)$; l_5 is a solution to $\Psi_{\mathrm{II}}(x, y) = \Psi_{\mathrm{III}}(x, y)$.

Since $\nabla\Psi_i(x, y)$ is not equal to zero inside Ω_i for $i = \mathrm{I}, \mathrm{II}, \mathrm{III}$, no stationary point of $\varpi(x, y)$ exists inside these sub-domains. Consequently, $\varpi(x, y)$ attains the global minimum only on the lines l_i $(i = 1, 2, \ldots, 5)$ and the boundary of Ω. By comparing the values of $\varpi(x, y)$ on the lines and the boundary, two optimal points in Ω, i.e., (x_0^*, y_0^*) intersected by l_1 and l_2, and (x_1^*, y_1^*) by l_3 and l_4, can be

expressed as

$$x_0^* = y_1^* = \frac{1}{2}\left(1 - \sqrt{2}\sqrt{\sqrt{2}-1}\right), \tag{A6}$$

$$x_1^* = y_0^* = \frac{1}{2}\left(1 + \sqrt{2}\sqrt{\sqrt{2}-1}\right). \tag{A7}$$

In such case, the minimum of $\varpi(x, y)$ is $(\sqrt{2}-1)^2/16$.

REFERENCES

1. Harrington, R. F., *Field Computation by Moment Methods*, IEEE Press, New York, 1993.
2. Rao, S. M., D. R. Wilton, and A. W. Glisson, "Electromagnetic scattering by surfaces of arbitrary shape," *IEEE Trans. Antennas Propag.*, Vol. 30, No. 3, 409–418, 1982.
3. Newman, E. H. and D. Forrai, "Scattering from a microstrip patch," *IEEE Trans. Antennas Propag.*, Vol. 35, No. 3, 245–251, 1987.
4. Newman, E. H., "Generation of wide-band data from the method of moments by interpolating the impedance matrix," *IEEE Trans. Antennas Propag.*, Vol. 36, No. 12, 1820–1824, 1988.
5. Virga, K. L. and Y. Rahmat-Samii, "Wide-band evaluation of communications antennas using $[Z]$ matrix interpolation with the method of moments," *Proc. IEEE AP-S Int. Symp.*, Vol. 2, 1262–1265, 1995.
6. Virga, K. L. and Y. Rahmat-Samii, "Efficient wide-band evaluation of mobile communications antennas using $[Z]$ or $[Y]$ matrix interpolation with the method of moments," *IEEE Trans. Antennas Propag.*, Vol. 47, No. 1, 65–76, 1999.
7. Barlevy, A. S. and Y. Rahmat-Samii, "An efficient method for wide band characterization of periodic structures using a modified Z matrix interpolation," *Proc. IEEE AP-S Int. Symp.*, Vol. 1, 56–59, 1997.
8. Barlevy, A. S. and Y. Rahmat-Samii, "Characterization of electromagnetic band-gaps composed of multiple periodic tripods with interconnecting vias: Concept, analysis, and design," *IEEE Trans. Antennas Propag.*, Vol. 49, No. 3, 343–353, 2001.
9. Yeo, J. and R. Mittra, "An algorithm for interpolating the frequency variations of method-of-moments matrices arising in the analysis of planar microstrip structures," *IEEE Trans. Microw. Theory Tech.*, Vol. 51, No. 3, 1018–1025, 2003.

10. Zhou, H. X. and W. Hong, "Fast Generation of $[Z]$ matrix in the method of moments over a wide frequency band by means of Hermite polynomial interpolation," *Proc. Asia-Pacific Microw. Conf., APMC' 02*, Vol. 2, 1196–1199, Kyoto, Japan, Nov. 19–22, 2002.
11. Li, W.-D., H.-X. Zhou, W. Hong, and T. Weiland, "An accurate interpolation scheme with derivative term for generating MoM matrices in frequency sweeps," *IEEE Trans. Antennas Propag.*, Vol. 57, No. 8, 2376–2385, 2009.
12. Li, W.-D., H.-X. Zhou, and W. Hong, "A Hermite inter/extrapolation scheme for MoM matrices over a frequency band," *IEEE Antennas Wireless Propag. Lett.*, Vol. 8, 782–785, 2009.
13. Reddy, C. J., M. D. Deshpande, C. R. Cockrell, and F. B. Beck, "Fast RCS computation over a frequency band using method of moments in conjunction with asymptotic waveform evaluation technique," *IEEE Trans. Antennas Propag.*, Vol. 46, No. 8, 1229–1233, 1998.
14. Nie, X. C., N. Yuan, L. W. Li, and Y. B. Gan, "Fast analysis of RCS over a frequency band using pre-corrected FFT/AIM and asymptotic waveform evaluation technique," *IEEE Trans. Antennas Propag.*, Vol. 56, No. 11, 3526–3533, 2008.
15. Tong, C. M., W. Hong, and N. Yuan, "Simultaneous interpolation of RCS in both angular and frequency domains based on AWE technique," *Microw. Opt. Tech. Lett.*, Vol. 32, No. 4, 290–293, 2002.
16. Erdemli, Y. E., J. Gong, C. J. Reddy, and J. L. Volakis, "Fast RCS pattern fill using AWE technique," *IEEE Trans. Antennas Propag.*, Vol. 46, No. 11, 1752–1753, 1998.
17. Wang, S., X. Guan, D.-W. Wang, X. Ma, and Y. Su, "Fast calculation of wide-band responses of complex radar targets," *Progress In Electromagnetics Research*, Vol. 68, 185–196, 2007.
18. Ling, J., S.-X. Gong, S.-T. Qin, W.-T. Wang, and Y.-J. Zhang, "Wide-band analysis of on-platform antenna using MoM-PO combined with Maehly approximation," *Journal of Electromagnetic Waves and Applications*, Vol. 24, No. 4, 475–484, 2010.
19. Chen, Y., S. Yang, S. He, and Z.-P. Nie, "Fast analysis of microstrip antennas over a frequency band using an accurate MoM matrix interpolation technique," *Progress In Electromagnetics Research*, Vol. 109, 301–324, 2010.
20. Li, J., X. Wang, and T. Wang, "On the validity of born

approximation," *Progress In Electromagnetics Research*, Vol. 107, 219–237, 2010.

21. Hellicar, A. D., J. S. Kot, G. C. James, and G. K. Cambrell, "The analysis of 3D model characterization and its impact on the accuracy of scattering calculations," *Progress In Electromagnetics Research*, Vol. 110, 125–145, 2010.
22. Shi, Y. and C. H. Chan, "Solution to electromagnetic scattering by bi-isotropic media using multilevel Green's function interpolation method," *Progress In Electromagnetics Research*, Vol. 97, 259–274, 2009.
23. Gustafsson, M., "Accurate and efficient evaluation of modal Green's functions," *Journal of Electromagnetic Waves and Applications*, Vol. 24, No. 10, 1291–1301, 2010.
24. Kim, B.-C., K.-K. Park, and H.-T. Kim, "Efficient RCS prediction method using angular division algorithm," *Journal of Electromagnetic Wave and Applications*, Vol. 23, No. 1, 65–74, 2009.
25. Park, K.-K. and H.-T. Kim, "RCS prediction acceleration and reduction of table size for the angular division algorithm," *Journal of Electromagnetic Wave and Applications*, Vol. 23, No. 11–12, 1657–1664, 2009.
26. Illahi, A. and Q. A. Naqvi, "Study of focusing of electromagnetic waves reflected by a PEMC backed chiral nihility reflector using Maslov's method," *Journal of Electromagnetic Wave and Applications*, Vol. 23, No. 7, 863–873, 2009.
27. See, K. Y., E. K. Chua, and Z.-H. Liu, "Accurate and efficient evaluation of MoM matrix based on a generalized analytical approach," *Progress In Electromagnetics Research*, Vol. 94, 367–382, 2009.